1    **Target localization optimization of a superstructure triple-column extractive**

2    **distillation with four-parallel evaporator organic Rankine cycles system based on**

3    **advanced exergy analysis**

4    Binhan Yuan [a,b], Zhenning Yang [c], Ao Yang [a,b,d], Jiqiang Tao [e], Jingzheng Ren [d],

5    Shun'an Wei [a,b,*], and Weifeng Shen [a,b,*]

6    [a] School of Chemistry and Chemical Engineering, Chongqing University, Chongqing

7    400044, People's Republic of China

8    [b] Chongqing Key Laboratory of Theoretical and Computational Chemistry, PR China

9    [c] Chongqing Changfeng Chemical Industrial Co., Ltd., Chongqing 401252, China

10   [d]Department of Industrial and Systems Engineering, Hong Kong Polytechnic

11   University, Hong Kong SAR, People's Republic of China

12   [e] Chongqing Unisplendour Chemical Co., Ltd., Chongqing 401252, China

13

14   **\*Corresponding Author:**

15   E-mail: wsacn@cqu.edu.cn (S. Wei) or shenweifeng@cqu.edu.cn (W. Shen)

16

17   **Abstract:** The energy analysis and optimization of process system aiming to solve the

18   problems of high consumption, low efficiency and unreasonable use of energy in the

19   process of energy utilization has been widely researched and developed in recent

20   decades. In this work, advanced exergy analysis was carried out for the triple-column

21   extractive distillation (TCED) process separating ternary azeotropic mixture of

22   ACN/EtOH/H2O. The total exergy destruction is 1097.69 KW. The avoidable exergy

23   destruction, is 29.20%, mainly caused by the cooler and three condensers. Based on the

24   thermodynamic analysis results, a superstructure TCED with four-parallel evaporator

25    organic Rankine cycles (FPE-ORC) system is proposed, four working fluids were

26    selected. An improved genetic algorithm is used to obtain the optimal operating

27    parameters of the ORC system by using the exergy efficiency and annual net profit

28    (ANP) of the ORC as two conflict objective functions. Compare with existing process,

29    the FPE-ORC system with working fluid R600 provides the highest exergy efficiency

30    of 12.27%, with working fluid R600a leads to the best economic benefit of 6.43 E+4

31    dollar/year.

34

## 1. Introduction

Distillation is commonly used in industry as a high-energy intensive separation process, and it requires extensive energy to achieve specified product purities [1]. The distillation related processes account for 10–15% of the world's energy consumption [2]. Thus, improving energy efficiency of distillation is expected to achieve greatest energy saving potential in the chemical industry. However, distillation column works like a heat engine with poor efficiency which does not consume heat but degrades it [3]. The inability to use the released low- grade heat is the main cause of energy expenditure [4]. As such, efficient use of low grade heat of the distillation process and improve its thermodynamic efficiency is the interest of this study.

Organic Rankine Cycle (ORC) is a mean of recovering waste heat which utilizes medium- and low-grade heat sources to generate electric power using the organic fluid as working medium, and it has great significance to improve the energy utilization efficiency. Liu *et al*. [5] presented a superstructure which combines methanol-to-gasoline (MTG) process with ORC to improve energy efficiency, and the novel structure saves cooling water by 18.77% and increases the thermal efficiency by 18.3% as compared with the industrial counterpart process. Yang *et al*. [6] reported a diethyl carbonate (DEC) process combining ORC to the heat pump-reactive dividing wall column (HP-RDW). The results illustrated that total annual cost of the HP-RDWC integrated ORC processes with working fluids R123 and R600a could be reduced by 11.78% and 10.30%, respectively. Li *et al*. [7] proposed a novel extractive distillation

56    process by combining economizer and ORC to effectively use the heat duty of

57    condenser. According to the above listed studies, the low-temperature waste heat could

58    be effectively recovered via the ORC system.

59        Exergy analysis, based on the second law of thermodynamics, is a method of

60    measuring the quality and efficient use of energy and providing much valuable

61    information [8]. The amount of exergy loss could be significantly reduced by adjusting

62    operating parameters [9]. Kaibel [10] and Ognisty [11] investigated the thermodynamic

63    analysis techniques for distillation columns and point out that exergy analysis is an

64    important tool for improving the thermodynamic performance and efficiency of the

65    column. In the study of Wang $et$ $al$. [12], the exergy analysis is applied to the proposed

66    process of synthesizing syngas with the triple $CO_2$ feeds to further find the optimal

67    matching scheme achieving significant energy reduction with pinch analysis.

68        Advanced exergy analysis (AEA) is an analysis method dividing exergy

69    destruction into four parts of endogenous, exogenous, avoidable and unavoidable [13],

70    which is superior to conventional exergy analysis (CEA). Not only it can clearly show

71    the cause of exergy loss, but also can clearly segment the system's avoidable exergy

72    destruction based on technical and economic constraints. Yan $et$ $al$. [14] proposed a new

73    process of Fischer-Tropsch synthesis combines with the dual-pressure ORC scheme

74    based on the AEA method. The result illustrated that the exergy destruction of the

75    proposed scheme is reduced from 34.92MW to 13.21MW, and 88.21% of the waste

76    heat source is recovered from the avoidable endogenous exergy destructions. Li $et$ $al$.

77 [15] carried out AEA on the performance of AFB gasification process. The result shows

78 that the exergy efficiency of the AFB gasification process is 82.13% and the total exergy

79 destruction is 4670 KW, and thereby 54.18% of the total exergy destruction can be

80 avoided. This strategy was also studied by Mohammadi *et al*. [16] for evaluating the

81 recompression supercritical $CO_2$ cycle. The result showed that the total exergy

82 efficiency of the system under real and unavoidable conditions is determined to be

83 16.63% and 17.13%, respectively. The maximum improvement potential, the avoidable

84 exergy destruction, for the system accounts for 50% of the total exergy destruction, and

85 of this avoidable value, and among which 34.59% is endogenous and 65.41% is

86 exogenous.

87 Although the exergy analysis approach has been widely used in distillation process,

88 to the best of our knowledge, previous studies mainly focuses on the overall

89 thermodynamic efficiency and ideal work required to complete common distillation

90 processes, valuable insights on the application of advanced exergy analysis to complex

91 distillation processes such as TCED have not yet been reported.

92 In this work, the advanced exergy analysis is introduced to accurately orientate the

93 locations of high-energy consumption of the triple-column extractive distillation, and

94 the energy-utilization optimization for target localization of this complex process is

95 carried out to achieve further waste heat recovery. The high-energy consumption parts

96 of this distillation system are accurately located via capturing the relationships of the

97 exergy destruction which caused by the interaction between different components. The

98 exergy destruction of the single column component is obtained by the calculation of the

99 stage-to-stage exergy balance. Significantly, to further reduce system exergy

100 destruction and improve system exergy efficiency, based on both conventional and

101 advanced exergy analysis, we propose a four parallel evaporators composite ORC

102 system (FPE-ORC) considering the interaction of multi-layer systems, and it is thereby

103 convenient for the optimization of entire system synchronously. Moreover, compared

104 to four independent ORC systems, this structure can meet the heat recovery and the

105 demand for equipment is the least at the same time, which can effectively reduce the

106 equipment investment cost. In addition, an improved genetic algorithm is used to obtain

107 the optimal operating parameters of the ORC system with the exergy efficiency and

108 annual net profit (ANP) of the ORC as two conflict objective functions.

109 **2. The existing TCED process for the separation of ACN/EtOH/H$_2$O ternary**

110 **azeotropic mixture**

111 Acetonitrile (ACN) and Ethanol (EtOH) are frequently applied as a mobile phase

112 in high performance liquid chromatography producing ACN/EtOH/water mixture. In

113 this work, the existing TCED configuration for separating ternary azeotropic mixture

114 of ACN/EtOH/H$_2$O proposed by Sun *et al*. [17] has been reproduced. This process is

115 achieved by two extractive distillation columns (i.e., EDC1 and EDC2) and an

116 entrainer-recovery column (i.e., ERC), as is presented in Fig. 1, the entrainer is

117 recovered from the bottom of ERC as a circulating stream and it is then sent to EDC1

118 and EDC2, respectively. 99.9 mol% of ACN, EtOH, and H$_2$O are obtained at the top of

119    EDC1, EDC2 and ERC, respectively.
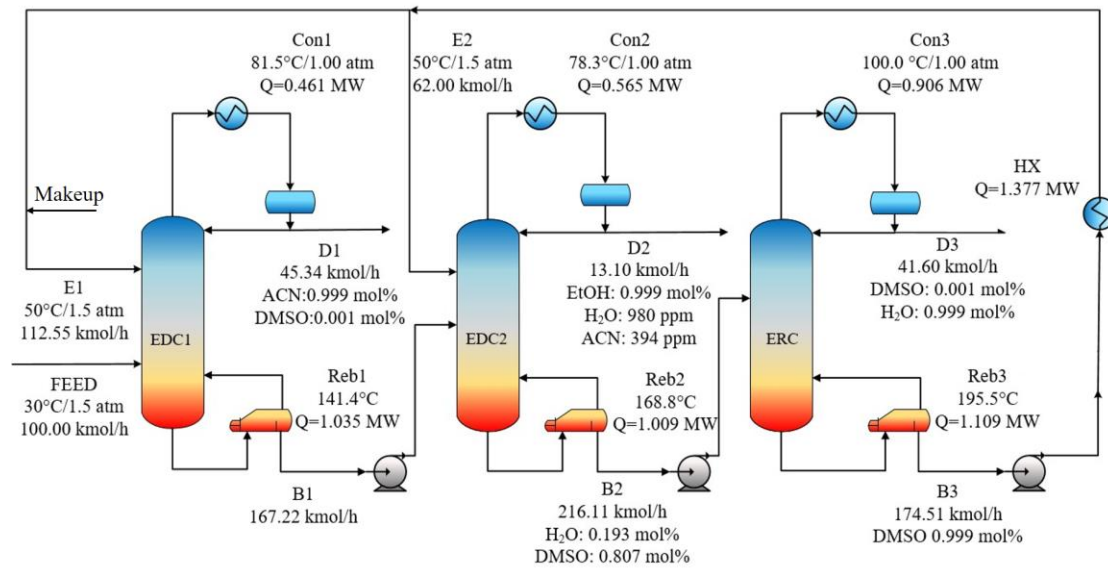


120

121    **Fig 1.** The existing TCED process for separating ternary azeotropic mixture of

122                                ACN/EtOH/H$_2$O

123    **3. Methodology**

124        A systematic procedure involving the thermodynamic analysis, conceptual design

125    of energy-saving framework and improved multi-objective optimization of TCED

126    process is shown in Fig 2, and the proposed approach is conducted in four steps:

127    (1) CEA method is used to analyze the TCED process theoretically.

128    (2) AEA method is used to analyze the TCED process theoretically.

129    (3) Conceptual design of a superstructure TCED with FPE-ORC system are proposed

130        to reduce avoidable exergy destruction, and four working fluids are selected.

131    (4) The improved genetic algorithm is adopted to optimize the ORC system by using

132        multiple objectives of annual net revenue and ORC exergy efficiency.

133
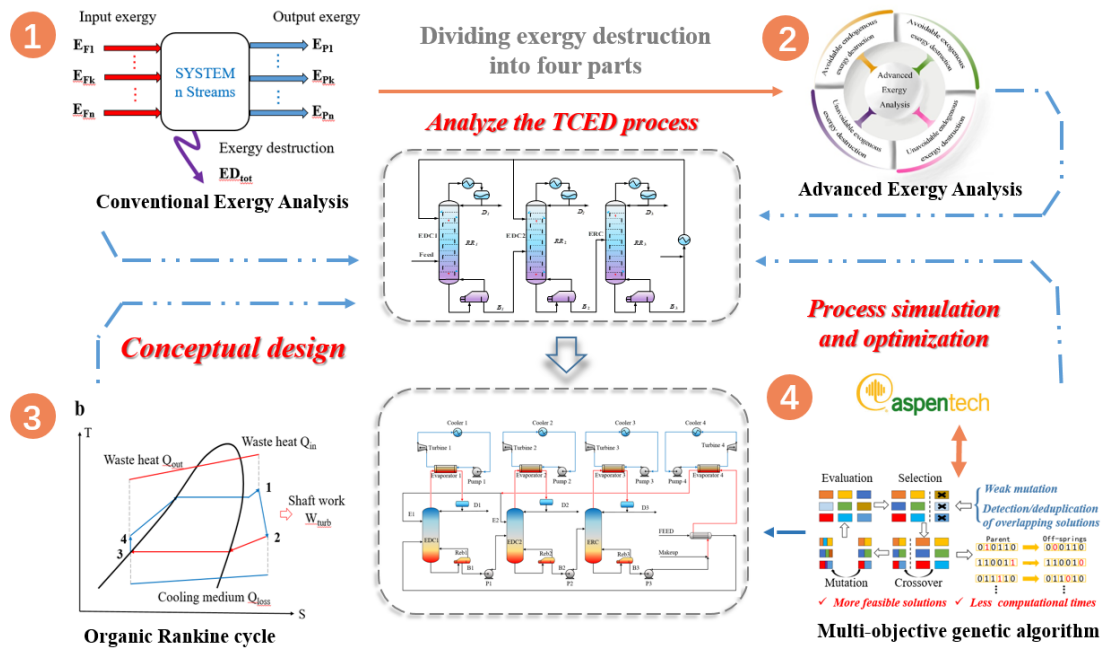
**Fig 2.** The proposed procedure based on thermodynamic analysis, conceptual design of energy-saving framework and improved multi-objective optimization of TCED process

**3.1. Conventional exergy analysis**

The second law of thermodynamics states that the part of energy called exergy or effective energy could theoretically be converted into useful work in the surrounding environment [18]. In any irreversible process, the amount of exergy decreases is referred to as exergy destruction [19]. The reference state of the environment in this study is defined as 25°C and 1.013 bar [20]

3.1.1 The exergy analysis of distillation column without condenser and reboiler

The process of mass transfer and heat transfer between vapor and liquid on each tray is irreversible, which must be accompanied by exergy destruction [21]. The mass, energy and exergy balance on a single tray *n* in the distillation column are shown in the Fig 3.

Stage *n*
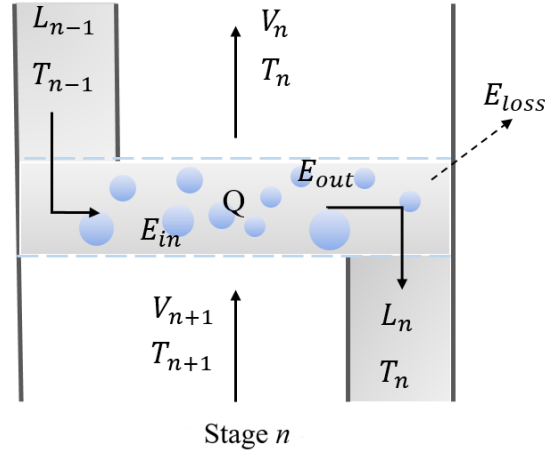
149

150          **Fig 3.** The mass, energy and exergy balance on a single tray

151          It is proved that exergy loss is correlated with entropy production in distillation by

152   the Gouy-Stodola theorem [22].

153   $$E_x^{loss} = T_0 \frac{dS^{irr}}{dt} \tag{1}$$

154          Suppose the microelement heat transfer between two import flows is δQ. The

155   temperature $T_{n+1}$ of vapor phase flow $V_{n+1}$ is higher than the temperature $T_{n-1}$ of

156   liquid phase flow $L_{n-1}$, thus the entropy loss caused by heat transfer in this process is

157   and is defined as **Equation (2)**[23].

158   $$dS = \delta Q(\frac{T_{n+1} - T_{n-1}}{T_{n+1}T_{n-1}}) \tag{2}$$

159          The exergy destruction due to heat transfer on a single column plate is defined as:

160   $$dE_D = T_0 \delta Q(\frac{T_{n+1} - T_{n-1}}{T_{n+1}T_{n-1}}) \tag{3}$$

161          The main driving force of the vapor-liquid mass transfer process in the distillation

162   column is the chemical potential difference of each component in the vapor-liquid flows.

163   Therefore, the exergy destruction on a tray caused by the mass transfer process can be

164     expressed as **Equation (4)** [24]:

165     $$dE_D = -RT_0 \sum_{i=1}^{k} \ln(\frac{a_i^{\alpha}}{a_i^{\beta}})dn_i \tag{4}$$

166     where, $a_i^{\alpha}$ and $a_i^{\beta}$ represent the activity of component $i$ in the vapor and liquid phase,

167     respectively.

168     3.1.2 Calculation of system exergy destruction

169     The exergy balance of a system is investigated to analyze the degradation of

170     energy by calculating the exergy value of every input or output stream [25]. The exergy

171     destruction indicating the loss of energy quality in an open thermodynamic system is

172     expressed in Equation (5) [14]:

173     $$E_{F,tot} = E_{P,tot} + E_{D,tot} \tag{5}$$

174     where, $E_{D,tot}$, $E_{F,tot}$, $E_{P,tot}$ refer to the exergy destruction, the input exergy, and the

175     output exergy of the overall system, respectively.

176     To explore the exergy loss distribution of the overall system, the exergy destruction

177     of each equipment should be initially calculated. For the kth component, it can be

178     calculated by Equation (6) [26, 27]:

179     $$E_{F,k} = E_{P,k} + E_{D,k} \tag{6}$$

180     where, $E_{D,k}$, $E_{F,k}$ and $E_{P,k}$ represent the exergy destruction, the input exergy, and the

181     output exergy of the kth equipment, respectively.

182     In addition, exergy efficiency and exergy destruction ratio indicate the efficiency

183     of the fuel exergy conversion into that of product and the reduction in the total

184     efficiency associated with thermodynamic inefficiency [28], which can calculate by Eqs.

185    (7-9) [29].

$$\varepsilon_k = \frac{E_{P,k}}{E_{F,k}} \times 100\% = (1 - \frac{E_{D,k}}{E_{F,k}}) \times 100\% \tag{7}$$

186

$$y_k = \frac{E_{D,k}}{E_{F,tot}} \times 100\% \tag{8}$$

187

$$y_k^* = \frac{E_{D,k}}{E_{D,tot}} \times 100\% \tag{9}$$

188

189    where $y_k$, and $y_k^*$ represent the ratio of total system exergy destruction to total fuel

190    and the ratio of exergy destruction within kth equipment to total exergy destruction of

191    the system respectively. $\varepsilon_k$ is used to assessment the efficiency of kth equipment in

192    energy conversion.

193    **3.2. Advanced exergy analyses**

194    AEA can estimate the interaction between different components of the same

195    system by dividing the exergy destruction of the components of the system into

196    endogenous/exogenous and avoidable/unavoidable.

197    3.2.1. Exogenous exergy destruction and endogenous exergy destruction

198    Endogenous exergy destruction ($E_{D,k}^{EN}$) refers to the part of exergy destruction

199    inside a component when other components are operating in an idealized state and the

200    considered component is operating at the same efficiency as the actual system. The

201    difference value between the exergy destruction and the endogenous part in the actual

202    system is the exogenous exergy destruction ($E_{D,k}^{EX}$), as it shown in Eq.10 [30].

$$E_{D,k} = E_{D,k}^{EN} + E_{D,k}^{EX} \tag{10}$$

203

204    3.2.2. Avoidable exergy destruction and unavoidable exergy destruction

205        The avoidable exergy destruction ($E_{D,k}^{AV}$) refers to the irreversibility part of exergy

206    destruction that can be reduced, which should be considered during the process

207    improvement. The unavoidable exergy destruction ($E_{D,k}^{UN}$) cannot be reduced owing to

208    economic and technological limitations such as the cost of materials and the feasibility

209    of manufacturing processes. It is calculated by Eq. (11). [31]

210    $E_{D,k} = E_{D,k}^{UN} + E_{D,k}^{AV}$                                       (11)

211        The modified exergetic efficiency $\varepsilon_k^*$ for avoidable exergy destruction in the kth

212    component can be defined as [32]

213    $\varepsilon_k^* = \dfrac{E_{P,k}}{E_{F,k} - E_{D,k}^{UN}} \times 100\% = (1 - \dfrac{E_{D,k}^{AV}}{E_{F,k} - E_{D,k}^{UN}}) \times 100\%$                    (12)

214    3.2.3. Combining the splitting methods

215        As a consequence of definitions in Eqs (8) and (9), the exergy destruction in the

216    kth component can be divided into four parts (Fig 4).

217    $E_{D,k} = E_{D,k}^{AV,EN} + E_{D,k}^{AV,EX} + E_{D,k}^{UN,EN} + E_{D,k}^{UN,EX}$            (13)



218

219            **Fig 4.** Partition of the exergy destruction within the kth equipment

220    Where, $E_{D,k}^{AV,EN}$ is the part of the avoidable irreversibility and can be avoided by

221    enhancing the kth component's efficiency. $E_{D,k}^{AV,EX}$ refers to the avoidable exogenous

222    exergy destruction that can be reduced by optimizing other equipment. $E_{D,k}^{UN,EN}$ and

223    $E_{D,k}^{UN,EX}$ respectively refer to the unavoidable portion of the endogenous and exogenous

224    irreversibility in the kth equipment that cannot be reduced due to the limitation of

225    technique and economy conditions. The above splitting combinations can be calculated

226    by Eq. (14-18) [33].

227    $$E_{D,k}^{AV} = E_{D,k} - E_{D,k}^{UN} \qquad (14)$$

228    $$E_{D,k}^{UN,EN} = E_{P,k}^{EN} \times (E_{P,k}^{D,k})^{UN} \qquad (15)$$

229    $$E_{D,k}^{UN,EX} = E_{D,k}^{UN} - E_{D,k}^{UN,EN} \qquad (16)$$

230    $$E_{D,k}^{AV,EN} = E_{D,k}^{EN} - E_{D,k}^{UN,EN} \qquad (17)$$

231    $$E_{D,k}^{AV,EX} = E_{D,k}^{EX} - E_{D,k}^{UN,EX} \qquad (18)$$

232    **3.3. Conceptual design of the proposed alternative configurations**

233    Large amount of low-temperature waste heat needs to be recovered to reduce

234    exergy destruction of whole system based on the analysis results. The ORC system is a

235    suitable approach which has four components – an evaporator, a turbine, a condenser

236    and a pump [34] as illustrated in Fig. 5 (a), and the corresponding T-S diagram is shown

237    in Fig. 5(b). The working fluid enters the turbine and leaves as a low pressure fluid to

238    generate electricity (point 1 to 2). The steam from the steam turbine gives off heat at

239    equal pressure in the condenser and condenses into a saturated liquid (point 2 to 3). The

240    condensed fluid is pressurized in the pump (point 3 to 4) and then enters the evaporator

241    for heat exchange with the waste heat stream under constant pressure (point 4 to 1). In

242    the evaporator, the working fluid goes through three stages: preheating, evaporation and

243    overheating.
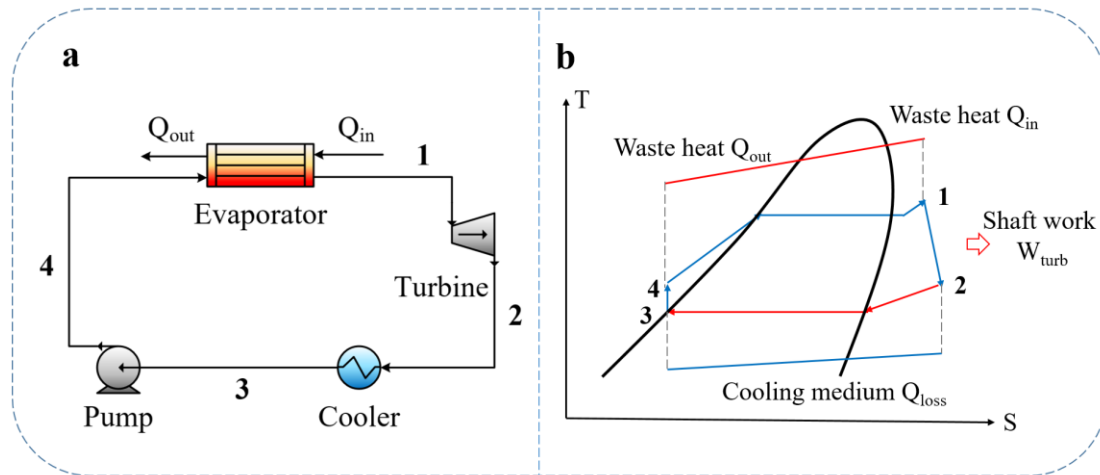


245    **Fig 5.** (a) Basic ORC system and (b) T–S diagram of an organic working fluid

246    In this study, a conceptual design scenario as shown in Fig 6 are put forward due

247    to it considered the interaction of multi-layer systems so as to simultaneously optimize

248    the whole structure. Moreover, compared to four independent ORC systems, this

249    structure can meet the heat recovery and the demand for equipment is the least at the

250    same time, which can effectively reduce the equipment investment cost.
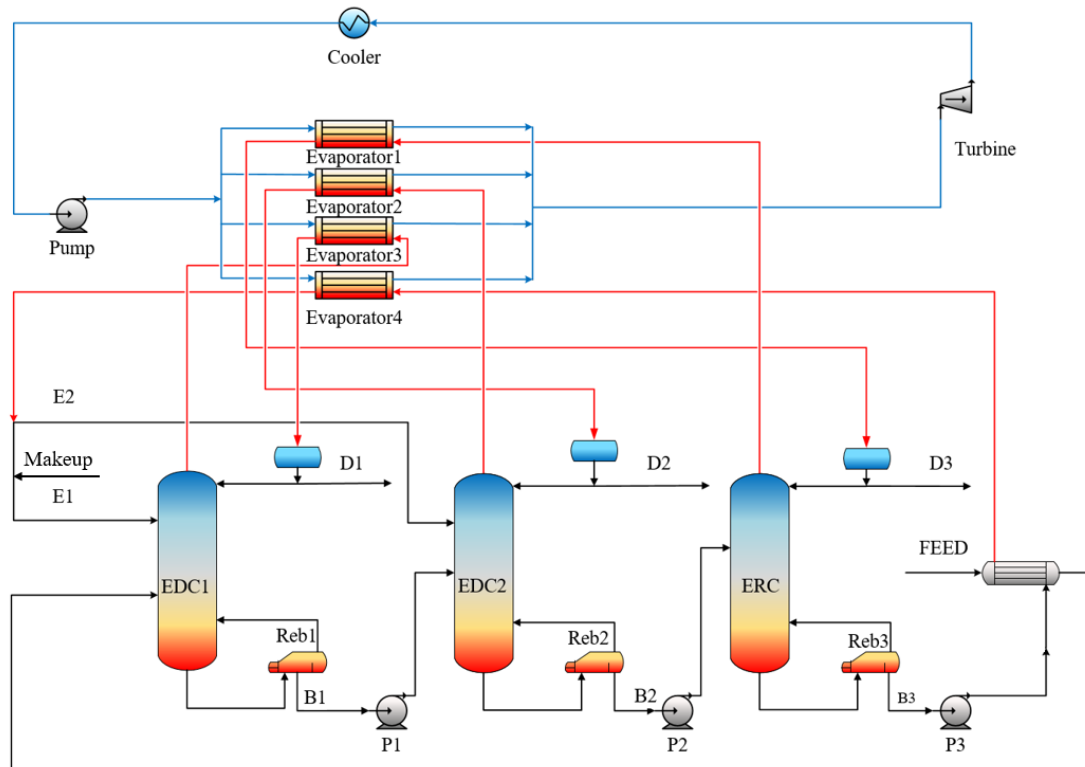
**Fig 6**. The alternative conceptual design scenario

Most of the waste heat sources are latent heat and suitable working fluid can achieve better heat matching. Thus, the selection of working fluids is a crucial step [35]. According to the slope of saturated steam curve, the working fluid can be divided into dry fluid, isentropic fluid, and wet fluid [36]. Dry working fluid and isentropic fluid are preferred because wet working fluids produce a few droplets during the expansion process, damaging turbine blades and reducing isentropic efficiency. It is noteworthy that it is impossible only consider single thermodynamic efficiency, other properties (e.g., the ozone depletion potential and global warming potential) also need to consider.

**3.4. Multi-objective optimization**

Herein, ASPEN Plus (V11.1) coupled an improved GA are used to obtain the optimal operating parameters of the FPE-ORC system by using two conflicting

264  objectives. The purpose of this study is to find an energy-saving scheme with low

265  exergy loss and considerable economic efficiency from the TCED process, therefore

266  the exergy efficiency and annual net profit (ANP) are selected as the confrontation

267  function.

268  $Maxf_1$ = annual net profit

269  $Maxf_2$ = ORC exergy efficiency

270     Objective function calculation is carried out in Aspen Plus and constraint condition

271  evaluation is executed in improved GA (see Fig.7). In the optimization process, the

272  connection between the improved multi-objective genetic algorithm based on VB.NET

273  and Aspen Plus is achieved by Active X [37]. The input parameters (e.g., feed flow rate)

274  are firstly determined to import the optimization module. The range of the design

275  variables which were determined based on sensitivity analysis in Aspen Plus. The first

276  population then generated by the improved genetic algorithm as input is sent back to

277  Aspen Plus. Fitness function vectors are then generated via the calculation of objective

278  functions and constraints. This optimization procedure will find improved individuals

279  throughout the generations and generate a set of the Pareto-front that moving towards

280  the optimal solutions.

281
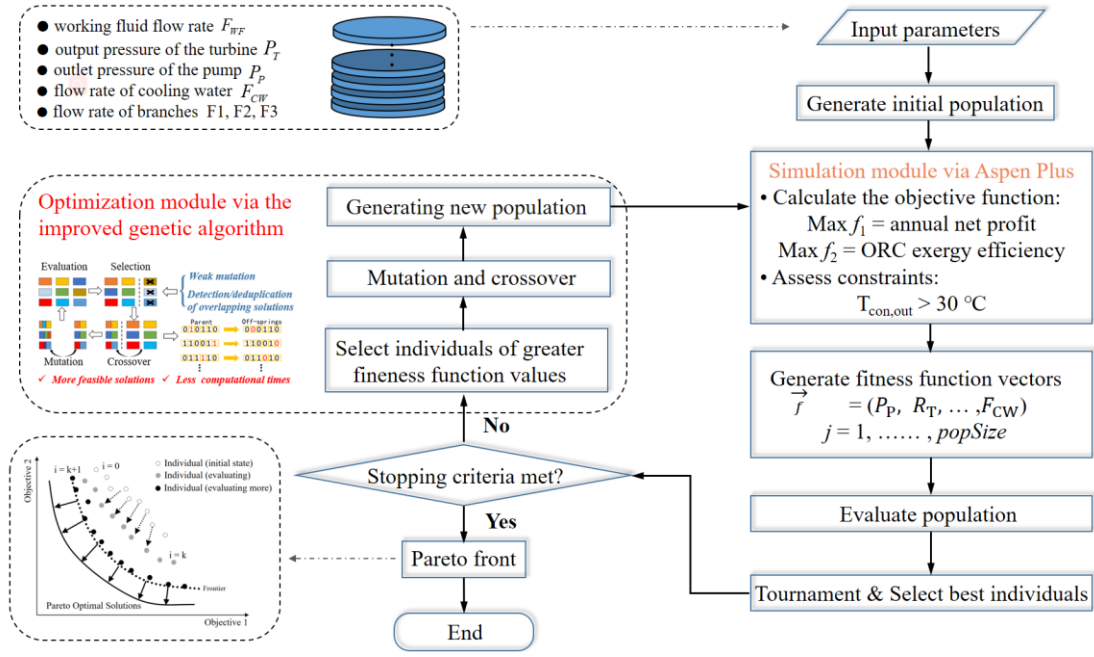
**Fig 7**. Scheme of the improved GA for the organic Rankine cycle

3.4.1 Objective function of ANP and exergy efficiency

In this study, total capital cost includes the fixed investment of a heat exchanger, four evaporators, a pump and a turbine, while the total energy investment involves the cost of electricity and cooling water. Capital cost of components and energy cost of cooling water and electricity are illustrated in Eqs. (19-24) [38-41].

$$\text{Capital cost of heat exchanger} = 9367.8 A_{exc}^{0.65} \tag{19}$$

$$\text{Capital cost of turbine} = 1.5 \times (225 + 170 \times V_{outlet}) \tag{20}$$

$$\text{Capital cost of evaporator} = 190 + 310 \times A_{eva} \tag{21}$$

$$\text{Capital cost of pump} = 900 \times (\frac{W}{300})^{0.25} \tag{22}$$

$$\text{Energy cost of cooling water} = 8000 \times PCW \times Q_{CW} \tag{23}$$

$$\text{Energy cost of electricity} = 8000 \times PE \times Q_{C} \tag{24}$$

where $V_{outlet} (m^3/s)$ is the outlet volumetric flow rate of the turbine. $A_{exc} (m^2)$

295 and $A_{eva}(m^2)$ represent the heat transfer area of the heat exchanger and the evaporator

296 respectively. Price of cooling water and electricity are defined as PCW (PCW = 0.354

297 US$/GJ) and PE (PE = 0.1 US$/KW·h) respectively. Heat duty of exchanger is

298 represented as $Q_{CW}$. Electricity consumption or generation of turbine and pump is

299 denoted as $Q_C$.

300      ANP for the ORC system is calculated by Eqs. 25 [42].

301 ANP = EOE - (capital cost of all equipment) /payback period      (25)

302 where EOE indicates earnings of electric, the payback period is assumed to be 5

303 years.[43]

304      The ORC exergy efficiency is defined as the ratio of the total exergy output to the

305 total exergy input.

306 $$\varepsilon_{ORC}^{tot} = \frac{E_{ORC}^{out}}{E_{ORC}^{in}} \times 100\% \qquad\qquad (26)$$

307 3.4.2 Constraint and variables bounds

308      According to the annual average climate temperature, the inlet temperature of

309 cooling water is 20 °C and the temperature rise is 10 °C [44]. To ensure that the working

310 fluid can be cooled by cooling water, the working fluid temperature at the cooler outlet

311 is limited to greater than 30 °C.

312      Herein, seven continuous variables—working fluid flow rate ($F_{WF}$), compression

313 ratio of the turbine ($R_T$), outlet pressure of the pump ($P_P$), flow rate of cooling water

314 ($F_{CW}$), and flow rate of branches (F1, F2, F3) —as shown in Eqs. (29)– (35) should be

315 optimized.

316 $$F_{WF}^{\min} \leq F_{WF} \leq F_{WF}^{\max} \tag{29}$$

317 $$F_{CW}^{\min} \leq F_{CW} \leq F_{CW}^{\max} \tag{30}$$

318 $$0 \leq F_1 \leq F_{WF} \tag{31}$$

319 $$0 \leq F_2 \leq F_{WF} \tag{32}$$

320 $$0 \leq F_3 \leq F_{WF} \tag{33}$$

321 $$R_T^{\min} \leq R_T \leq R_T^{\max} \tag{34}$$

322 $$P_P^{\min} \leq P_P \leq P_P^{\max} \tag{35}$$

323 **4. Results and discussion**

324 **4.1. Conventional exergy analyses of TCED**

325    Based on the simulation results of TCED process, the conventional exergy analysis

326 is carried out and the results are shown in Table 1. The input effective energy and output

327 effective energy of the whole process are 4979.31 KW and 3881.61KW respectively. It

328 is apparent that the maximum value of exergy destruction (235.599 KW) occurs in the

329 cooler (HX) resulting from the recycle entrainer stream is cooled by the cooling water.

330 Similarly, the condensers of EDC1, EDC2 and ERC also have great exergy destruction,

331 with exergy efficiencies of 34.76%, 33.94% and 26.32% respectively. There is a large

332 temperature difference between the top stream of the distillation column and the cooling

333 medium (cooling water) which is the main reason for plenty of the exergy destruction

334 in the condenser. As for other component, large heat transfer force (temperature

335 difference) and mass transfer force (chemical potential difference) for vapor-liquid

336 phase are the main reason of the exergy destruction in the distillation column, and small

337    exergy destruction is caused by the pumps due to the irreversibility.

338         **Table 1.** Computing results of the TCED processes based on CEA.

| Equipment | $E_{F,k}(KW)$ | $E_{P,k}(KW)$ | $E_{D,k}(KW)$ | $\varepsilon_k(\%)$ | $y_k(\%)$ | $y_k^*(\%)$ |
|---|---|---|---|---|---|---|
| Con1 | 87.40 | 30.38 | 57.01 | 34.76 | 1.15 | 5.19 |
| Con2 | 85.01 | 28.86 | 56.16 | 33.94 | 1.13 | 5.12 |
| Con3 | 203.37 | 53.53 | 149.84 | 26.32 | 3.01 | 13.65 |
| HX | 287.50 | 51.90 | 235.60 | 18.05 | 4.73 | 21.46 |
| Reb1 | 495.45 | 444.65 | 50.80 | 89.75 | 1.02 | 4.63 |
| Reb2 | 641.32 | 612.70 | 28.62 | 95.54 | 0.57 | 2.61 |
| Reb3 | 1147.94 | 1069.18 | 78.76 | 93.14 | 1.58 | 7.18 |
| P1 | 118.95 | 118.67 | 0.28 | 99.76 | 0.01 | 0.03 |
| P2 | 231.88 | 231.58 | 0.29 | 99.87 | 0.01 | 0.03 |
| P3 | 281.58 | 280.78 | 0.80 | 99.72 | 0.02 | 0.07 |
| EDC1 | 221.77 | 127.45 | 94.32 | 57.47 | 1.89 | 8.59 |
| EDC2 | 398.97 | 247.12 | 151.85 | 61.94 | 3.05 | 13.83 |
| ERC | 778.19 | 584.82 | 193.36 | 75.15 | 3.88 | 17.62 |
| TOT | 4979.31 | 3881.61 | 1097.69 | 77.95 | 22.05 | 100.00 |

339    **4.2. Advanced conventional exergy analyses of TCED**

340         The advanced exergy analysis integrates unavoidable and avoidable as well as

341    endogenous and exogenous exergy destruction to analyze the whole process

342    respectively. The unavoidable and theoretical operating parameters of the main

343    component are shown in Table 2 [14]. The results of all the equipment based on the

344    AEA are listed in Table 3, which can be concluded that endogenous exergy destruction

345    and exogenous exergy destruction are greatly different with different components. The

346    exogenous exergy destruction caused by the distillation column EDC1, DEC2 EDC3

347    are more than the other equipment because of the operation parameters reboiler and

348    condenser. It is noteworthy that from Fig. 8 that the 48.80% exergy destruction in whole

349    process is endogenous indicating that improving the interaction among the equipment

350  can increase the thermodynamic irreversibility of the whole process. In addition, the

351  51.20% exergy destruction in whole process is exogenous indicating it is necessary to

352  improve the performance and operation parameter of the equipment within high

353  exogenous exergy destruction (e.g., EDC1, EDC2 and ERC) and high endogenous

354  exergy destruction (e.g., condensers and exchanger HX) for the aim of energy saving.
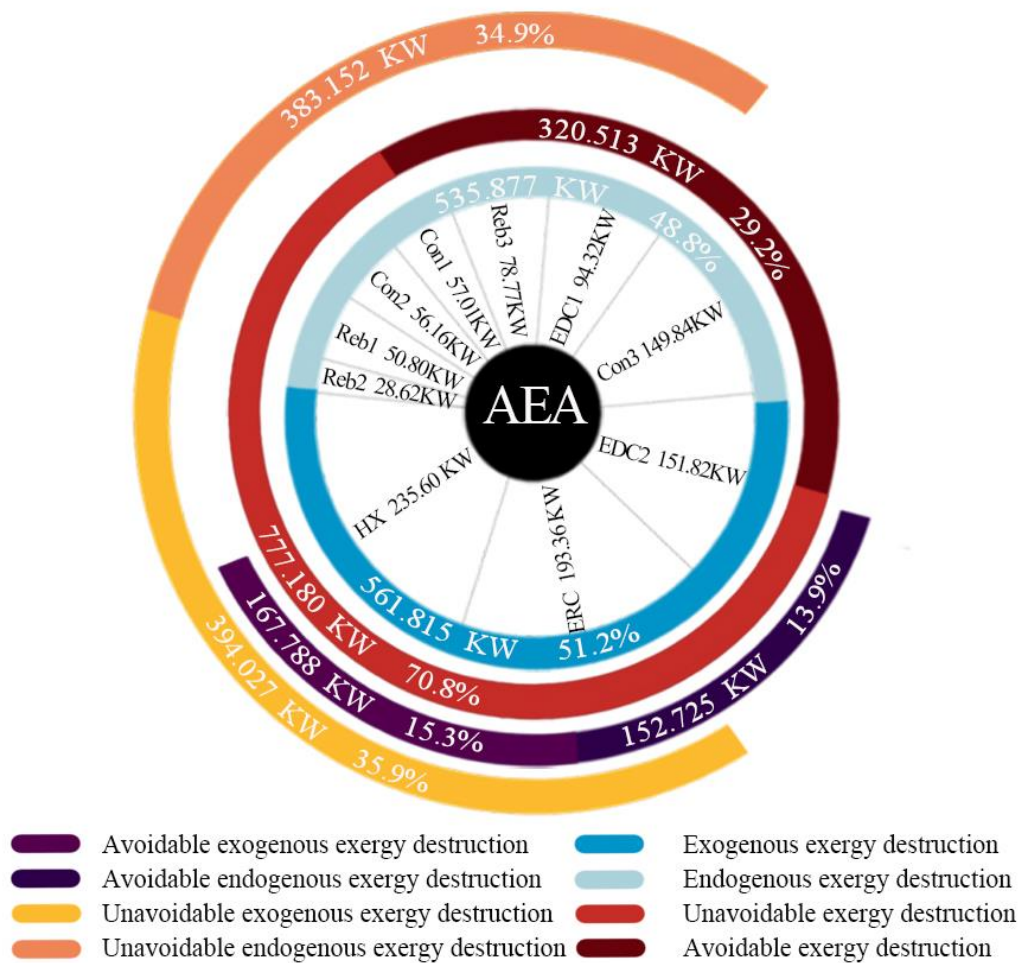


355

356  **Fig 8.** Division of total exergy destruction for separating ACN/EtOH/H2O ternary

357  azeotropic mixture by TCED

358  In this work, the results of the unavoidable/avoidable exergy destruction of the

359  different components are summarized in the fourth and fifth column of Table 3 and

360  described in Fig. 9. The system avoidable exergy destruction accounted for 29.20% of

361    whole system exergy destruction. The largest values of avoidable exergy 77.393 KW

362    are destructed in the EDC2, followed by Con3, EDC1. The avoidable exergy

363    destruction ratios of those three equipment are 50.96%, 49.02%, 76.89%, respectively

364    indicting great potential for improvement.

365        The total exergy destruction by using the combined splitting of endogenous and

366    exogenous as well as unavoidable and avoidable exergy destruction listed in the last

367    four columns of Table 3. Of concern is that avoidable endogenous exergy destruction

368    indicates the independent improvement potential of each component. As is evident in

369    Fig. 9, the Con3 has the largest avoidable endogenous exergy destruction, which is

370    73.454KW, followed by the Con1, Con2. Although the cooler HX has a large exergy

371    destruction value, the avoidable endogenous exergy destruction is small, and it does not

372    have a great energy-saving potential by improving the equipment's own parameters. In

373    addition, EDC2 generates the largest avoidable exogenous exergy destruction, which is

374    69.987KW, followed by the EDC1 and ERC. This means that efforts should be focused

375    on improving the performance of other components to reduce their exergy destruction.

376        **Table 2.** Condition assumptions of the unavoidable exergy destruction

| Equipment | Unavoidable condition |
| --- | --- |
| Heat changer | Minimum temperature approach =5.0 K |
| Pump | Isentropic efficiency= 90% |
| Distillation column without reboiler and Condenser | Equilibrium stage |

377        **Table 3.** Results of advanced exergetic analysis of TCED processes.

| Equip-ment | Exergy destruction (KW) | | | | | | | |
| --- | --- | --- | --- | --- | --- | --- | --- | --- |
| | $E_{D,k}^{EN}$ | $E_{D,k}^{EX}$ | $E_{D,k}^{UN}$ | $E_{D,k}^{AV}$ | $E_{D,k}^{UN,EN}$ | $E_{D,k}^{AV,EN}$ | $E_{D,k}^{UN,EX}$ | $E_{D,k}^{AV,EX}$ |

| | | | | | | | | |
|---|---|---|---|---|---|---|---|---|
| Con1 | 57.01 | 0.00 | 25.20 | 31.81 | 31.81 | 25.20 | 0.00 | 0.00 |
| Con2 | 56.16 | 0.00 | 24.26 | 31.90 | 31.90 | 24.26 | 0.00 | 0.00 |
| Con3 | 149.84 | 0.00 | 73.45 | 76.38 | 76.38 | 73.45 | 0.00 | 0.00 |
| HX | 235.60 | 0.00 | 8.51 | 227.09 | 227.09 | 8.51 | 0.00 | 0.00 |
| Reb1 | 2.21 | 48.59 | 3.41 | 47.38 | 2.12 | 0.09 | 45.26 | 3.33 |
| Reb2 | 0.90 | 27.71 | 1.22 | 27.40 | 0.87 | 0.04 | 26.53 | 1.18 |
| Reb3 | 1.42 | 77.34 | 0.40 | 78.36 | 1.33 | 0.09 | 77.03 | 0.31 |
| P1 | 0.05 | 0.24 | 0.15 | 0.13 | 0.02 | 0.03 | 0.11 | 0.13 |
| P2 | 0.03 | 0.27 | 0.14 | 0.15 | 0.01 | 0.01 | 0.14 | 0.13 |
| P3 | 0.06 | 0.75 | 0.40 | 0.40 | 0.03 | 0.03 | 0.38 | 0.37 |
| EDC1 | 14.32 | 80.00 | 72.52 | 21.80 | 2.13 | 12.19 | 19.67 | 60.33 |
| EDC2 | 11.89 | 139.96 | 77.39 | 74.46 | 4.48 | 7.41 | 69.97 | 69.99 |
| ERC | 6.40 | 186.97 | 33.44 | 159.92 | 4.97 | 1.42 | 154.95 | 32.02 |
| TOT | 535.88 | 561.82 | 320.51 | 777.18 | 383.15 | 152.72 | 394.03 | 167.79 |
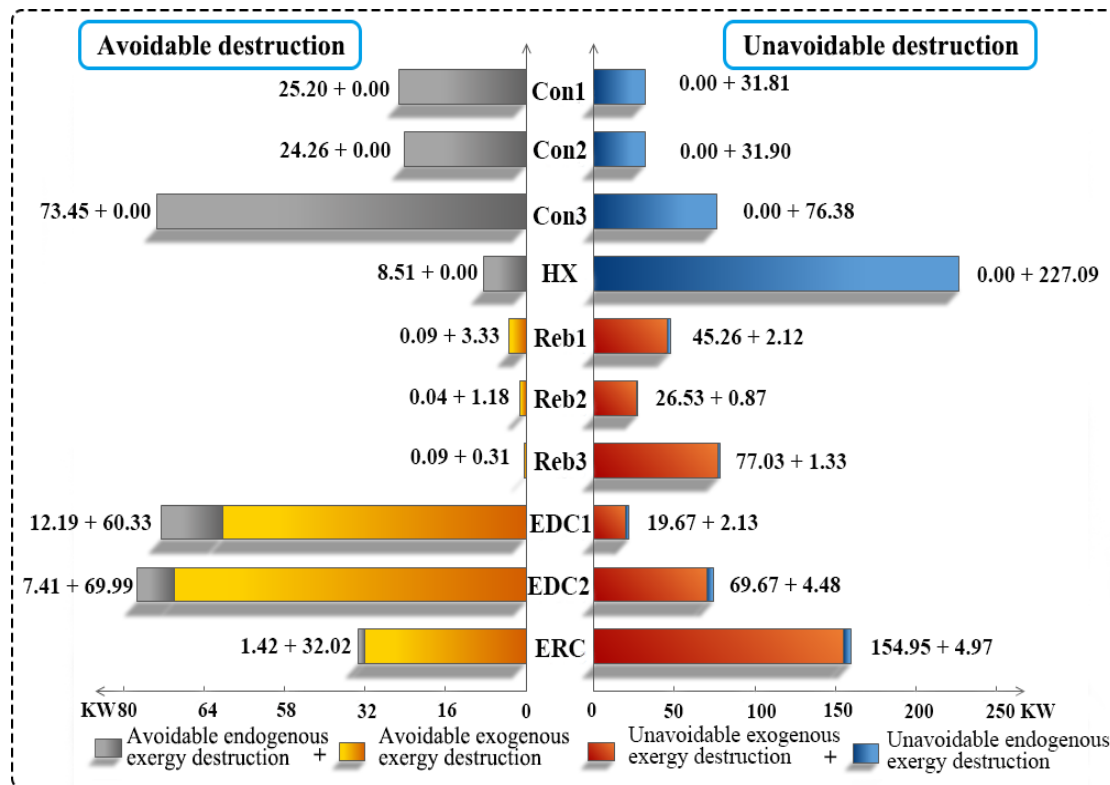


**Fig 9.** The cumulative bar chart of exergy destruction within the kth equipment

## 4.3. Conceptual design alternative configurations based on the analysis results

Based on the theoretical analysis results, the exergy destruction of distillation process in this study is mainly caused by the large temperature difference between the

384 top vapor stream of the distillation column and the cooling medium. To reduce exergy

385 destruction during the TCED process, more attention should be given to improve the

386 operating parameters of the three condensers and cooler HX.

387     In this study, an ORC system combine with four parallel evaporators is designed

388 to match four remaining heat sources. Significantly, the column has larger exergy

389 destruction when the rectifying section with saturated vapor feed and in the stripping

390 section with the saturated liquid feed. Hence by preheating or precooling the stream to

391 change the thermal parameters of the feedstock entering the distillation column, the

392 energy consumption and the effective energy loss in the column can be reduced. In this

393 work, the heat flow in cooler HX preheats the feed flow FEED first.

394     The thermodynamic efficiency, ozone depletion potential (ODP) and global

395 warming potential (GWP) are considered comprehensively. Four working fluids

396 candidates including R600, R600A, R601, R601A are chosen to the ORC system. The

397 detailed information is illustrated in Table 4. All the alternative working fluids have

398 lower ODP and GWP. The T-S diagrams of four working fluids are displayed in Fig. 10.

399 It can be seen from the slope of the T-S curve, the four working fluids are all dry
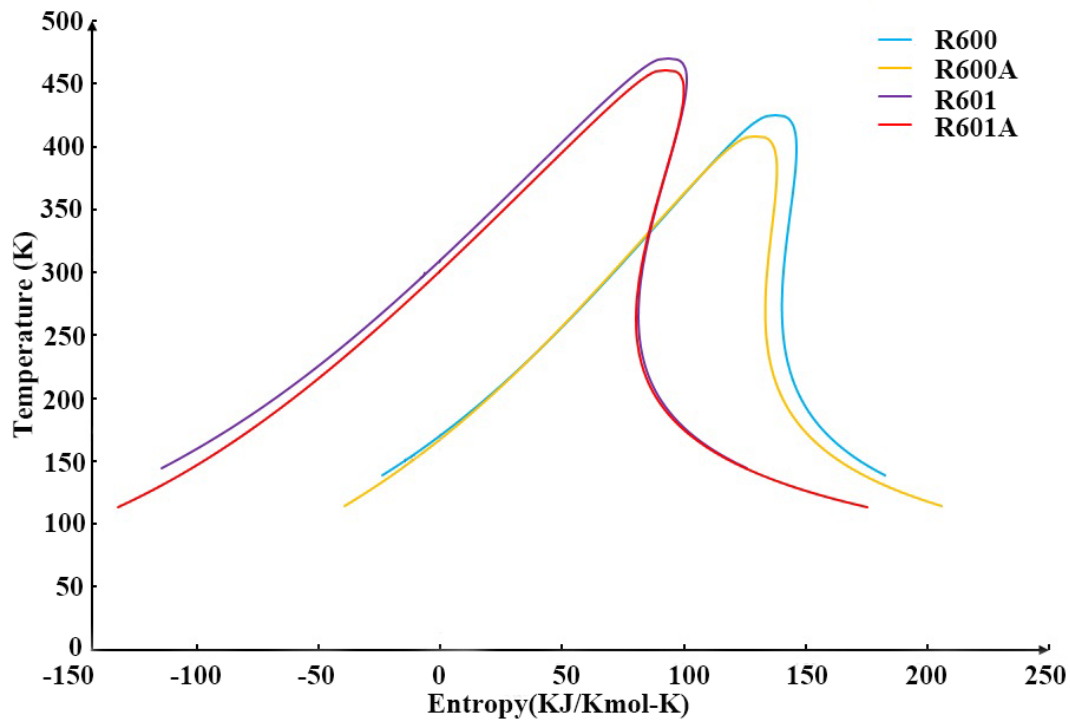
400 working fluids.

401                   **Table 4.** Properties of alternative organic working fluids

| Working fluid | R600 | R600A | R601 | R601A |
|---|---|---|---|---|
| Chemical formula | $C_4H_{10}$-1 | $C_4H_{10}$-2 | $C_5H_{12}$-1 | $C_5H_{12}$-2 |
| CAS No. | 106-97-8 | 75-28-5 | 109-66-0 | 78-78-4 |
| Critical temperature/ °C | 151.97 | 134.65 | 196.55 | 187.25 |
| Critical pressure/ atm | 37.96 | 36.4 | 33.7 | 33.8 |
| Vaporization heat/ $kJ \cdot kg^{-1}$ | 383.5 | 364.29 | 355.9 | 341.36 |

| | | | | |
|---|---|---|---|---|
| ODP[a] | 0.0 | 0.0 | 0.0 | 0.0 |
| GWP[b] [100year] | 20 | 20 | 20 | 20 |
| Type | dry | dry | dry | dry |

[a] ODP: ozone depletion potential, relative to R11

[b] GWP: global warming potential, relative to $CO_2$



**Fig 10.** T-S diagram of four working fluids (R600, R600A, R601, R601A).

## 4.4 The optimization results of the FPE-ORC system

The range of the design variables which were determined based on sensitivity analysis in Aspen Plus are presented in Tables 6a-d of the supporting information. The optimize parameters of improved GA are set to have an initial population of 100, a crossover probability of 0.95, and a mutation probability of 0.1. As illustrated in Fig. 11, the optimizations are respectively ended at 320 generations, 220 generations, 130 generations and 80 generations because the vector of decision variables has not made any meaningful improvement. Additionally, the optimal Pareto fronts between ANP and

414  exergy efficiency with four working fluids are shown in Fig. 12, respectively.
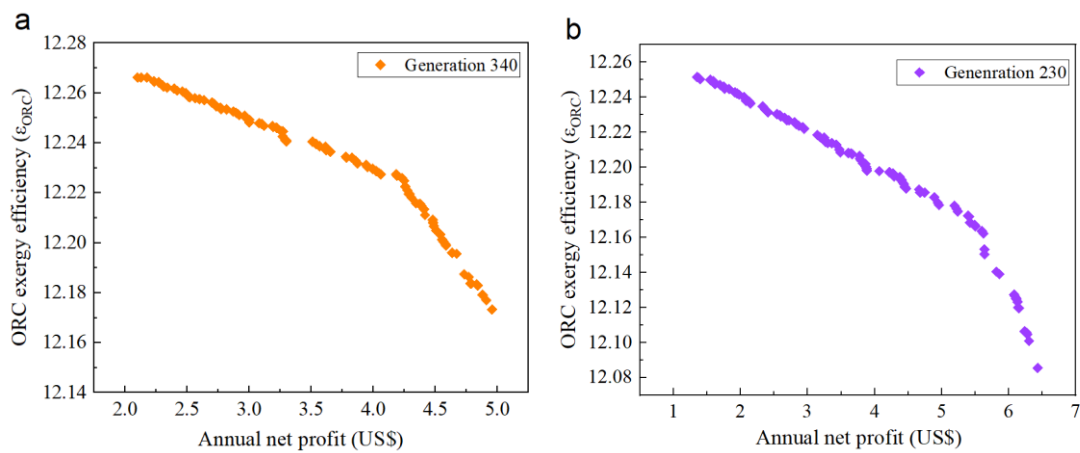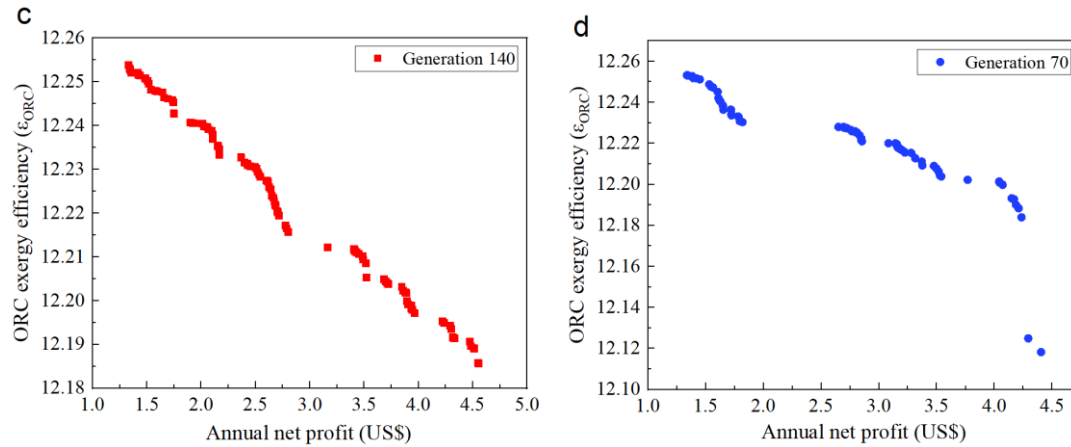


415

416
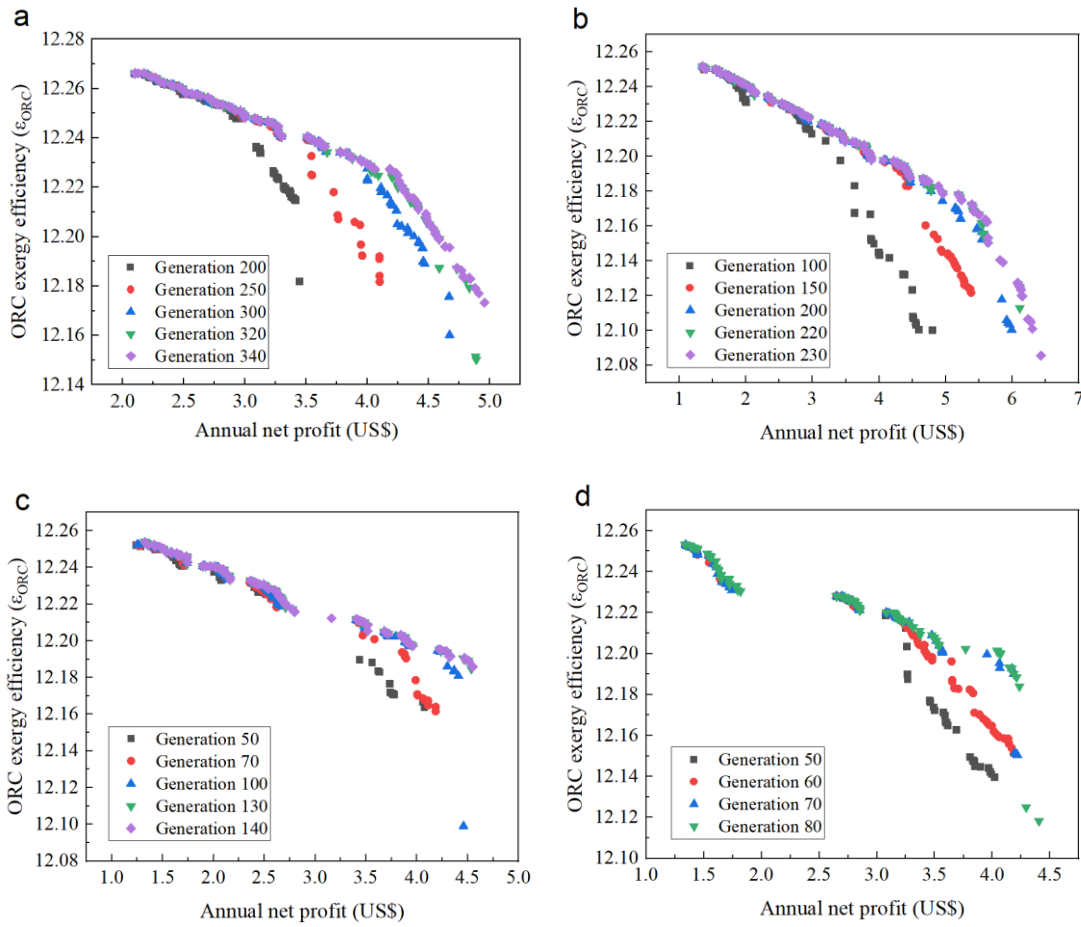
**Fig 11.** Multi-objective optimization of the FPE-ORC system with working fluid (a) R600, (b)R600A, (c) R601 and (d) R601A.

419



420

**Fig 12.** Pareto front solutions by using working fluid (a) R600 (b)R600A (c) R601 (d) R601A.

The Pareto fronts between ANP and exergy efficiency of four working fluids are shown in Fig. 12. Two solutions with highest net revenue solution and highest ORC efficiency solution are provided in this study, with the optimization results of decision variables and objective function are illustrating in Table 5a, b. The ORC system with working fluid R600a shows the best economic benefit of 6.43 E+4 dollar/year and the exergy efficiency is 12.09%. With working fluid R600 has the highest exergy efficiency 12.27% and ANP is 2.1 E+4 dollar/year. Compared to the total exergy destruction of the existing process, 79.31% of avoidable exergy destructions are decreased in the FPE-ORC scheme with working fluids of R600 and the exergy destruction of whole system is reduced from 1097.69 KW to 807.47 KW.

**Table 5a**. The optimization results of decision variables and objective function with the highest exergy efficiency

| Four working fluids conditions | R600 | R600A | R601 | R601A |
|---|---|---|---|---|
| $F_{WF}$ (kmol) | 329.47 | 285.97 | 281.26 | 375.49 |
| $R_T$ | 0.66 | 0.66 | 0.66 | 0.73 |
| $P_P$ (bar) | 4.48 | 1.84 | 1.73 | 6.44 |
| $F_{CW}$ (kmol)) | 10473.11 | 10559.77 | 10562.85 | 10562.93 |
| $F1$ (kmol) | 130.78 | 60.10 | 59.28 | 76.57 |
| $F2$ (kmol) | 71.79 | 63.27 | 62.68 | 79.83 |
| $F3$ (kmol) | 67.31 | 112.22 | 109.83 | 150.25 |

| ORC System exergy loss (KW) | 384.90 | 384.99 | 384.90 | 438.75 |
|---|---|---|---|---|
| Total exergy loss after configuration improvement (KW) | 983.98 | 984.07 | 983.98 | 1037.83 |
| ANP (10^4 dollar/year) | 2.10 | 1.35 | 1.33 | 1.34 |
| **Exergy efficiency (%)** | **12.27** | **12.25** | **12.25** | **12.25** |

436

437 **Table 5b** The optimization results of decision variables and objective function with

438 the highest economic benefits

| Four working fluids conditions | R600 | R600A | R601 | R601A |
|---|---|---|---|---|
| $F_{WF}$ (kmol) | 323.18 | 285.34 | 280.86 | 377.89 |
| $R_T$ | 0.52 | 0.4 | 0.47 | 0.59 |
| $P_P$ (bar) | 5.45 | 2.72 | 2.14 | 8.51 |
| $F_{CW}$ (kmol)) | 10341.21 | 10300.62 | 10344.65 | 10473.48 |
| $F1$ (kmol) | 127.62 | 60.30 | 59.29 | 76.49 |
| $F2$ (kmol) | 71.66 | 63.29 | 62.52 | 87.67 |
| $F3$ (kmol) | 67.55 | 111.86 | 102.25 | 150.03 |
| ORC System exergy loss (KW) | 395.28 | 397.84 | 394.26 | 441.93 |
| Total exergy loss after configuration improvement (KW) | 994.36 | 996.92 | 993.34 | 1041.01 |
| **ANP (10^4 dollar/year)** | **4.96** | **6.43** | **4.75** | **4.41** |
| Exergy efficiency (%) | 12.17 | 12.09 | 12.17 | 12.12 |

439 **5. Conclusions**

440 In this study, the advanced exergy analysis is used to explore the interaction

441 between different components of the triple-column extractive distillation to orientate

442 the locations of high-energy consumption. As it turned out, the avoidable exergy

443 destruction in the TCED process is mainly caused by the cooler and three condensers.

444 Based on the results, we propose a superstructure triple-column extractive

445 distillation with four-parallel evaporator organic Rankine cycles system, which

446 considering the interaction of multi-layer systems while reducing equipment

447    investment costs. Then, an improved genetic algorithm is used to obtain the optimal

448    operating parameters of the ORC system with the exergy efficiency and ANP as two

449    conflict objective functions. As compared with the existing process, the FPE-ORC

450    system with working fluids R600 has the best performance with highest exergy

451    efficiency and with working fluids R600a has the best economic benefit.

452       It is worth to mention that the advanced exergy analysis method and proposed

453    systematic scheme of extractive distillation integrated with ORC can be widely applied

454    to other processes even to the plant or industry zone. Moreover, the exergoeconomic

455    analysis can be explored to the process system for indicating economic effects

456    associated with exergy destruction of equipment.

461

462 **Nomenclature**

| | | | |
|---|---|---|---|
| a | activity | V | volumetric flow rate m$^3$/s |
| A | heat transfer area m$^2$ | y | exergy destruction ratio |
| ACN | acetonitrile | y* | relative exergy destruction |
| AEA | advanced exergy analysis | ε | exergy efficiency |
| ANP | annual net profit, dollar/year | | |
| CEA | conventional exergy analysis | *Subscripts* | |
| Con | condenser | C | electricity |
| DMSO | dimethyl sulfoxide | CW | cooling water |
| E | exergy, KW | D | destruction |
| EDC1 | extractive distillation columns 1 | F | feed |
| EDC2 | extractive distillation columns 2 | in | input |
| ERC | entrainer-recovery column | irr | irreversible |
| EtOH | ethanol | k | k-th equipment |
| EOE | earnings of electric, dollar/year | out | output |
| F | flow rate | P | pump |
| FPE-ORC | ORC combine with four parallel evaporator | P | product |
| GWP | global warming potential | T | turbine |
| H | enthalpy, kJ/mol | tot | total |
| HX | cooler | 0 | ambient state |
| i | component i | exc | heat exchanger |
| L | liquid | eva | evaporator |
| n | number | WF | working fluid |
| ODP | ozone depletion potential | | |
| ORC | Organic Rankine cycle | *Superscripts* | |
| P | pressure | AV | avoidable |
| P | pump | CH | chemical |
| PCW | Price of cooling water | EN | endogenous |
| PE | Price of electricity | EX | exogenous |
| Q | heat transfer rate (KW) | KN | kinetic |
| Reb | reboiler | max | maximum |
| S | entropy, kJ/(mol. K) | min | minimum |
| T | temperature, K | PH | physical |
| TAC | Total annualized cost, dollar/year | PT | potential |
| TCED | triple-column extractive distillation | UN | unavoidable |
| V | vapor | | |

463

464

**Reference**

[1] J. Liang, H. Zhou, J. Li, W. Kong, Z. Ma, L. Sun, Comparison of dynamic performances for heat integrated reactive distillation considering safety, Chemical Engineering and Processing - Process Intensification, 160 (2021) 108294.

[2] D.S. Sholl, R.P. Lively, Seven chemical separations to change the world, Nature, 532 (2016) 435-437.

[3] M. Blahusiak, A.A. Kiss, S.R.A. Kersten, B. Schuur, Quick assessment of binary distillation efficiency using a heat engine perspective, Energy, 116 (2016) 20-31.

[4] A.A. Kiss, R. Smith, Rethinking energy use in distillation processes for a more sustainable chemical industry, Energy, 203 (2020) 117788.

[5] S.Y. Liu, J. He, D.X. Lu, J.S. Sun, Optimal integration of methanol-to-gasoline process with organic Rankine cycle, Chem Eng Res Des, 154 (2020) 182-191.

[6] A. Yang, Y. Su, W.F. Shen, I.L. Chien, J.Z. Ren, Multi-objective optimization of organic Rankine cycle system for the waste heat recovery in the heat pump assisted reactive dividing wall column, Energ Convers Manage, 199 (2019) 112041.

[7] X.G. Li, C.T. Cui, H. Li, X. Gao. Process synthesis and simultaneous optimization of extractive distillation system integrated with organic Rankine cycle and economizer for waste heat recovery. J Taiwan Inst Chem E, 102 (2019) 102:61–72.

[8] A. Yang, L.P. Lv, W.F. Shen, L.C. Dong, J. Li, X. Xiao, Optimal Design and Effective Control of the tent-Amyl Methyl Ether Production Process Using an Integrated Reactive Dividing Wall and Pressure Swing Columns, Ind Eng Chem Res, 56 (2017) 14565-14581.

[9] J.S. Sun, F. Wang, T.T. Ma, H. Gao, P. Wu, L.L. Liu, Energy and exergy analysis of a five-column methanol distillation scheme, Energy, 45 (2012) 696-703.

[10] E.B.a.J.K. G. Kaibel, Thermodynamics-guideline for the development of distillation column arrangements, Gas Separation & Purification 4(1990) 109-114.

[11] T.P. Ognisty, Analyze Distillation-Columns with Thermodynamics, Chem Eng Prog, 91 (1995) 40-46.

[12] H. Wang, Y. Su, D. Wang, S.M. Jin, S.A. Wei, W.F. Shen, Optimal Design and Energy-Saving Investigation of the Triple CO2 Feeds for Methanol Production System by Combining Steam and Dry Methane Reforming, Ind Eng Chem Res, 59 (2020) 1596-1606.

[13] M. Fallah, S. Mohammad, S. Mahmoudi, M. Yari, R.A. Ghiasi, Advanced exergy analysis of the Kalina cycle applied for low temperature enhanced geothermal

499      system, Energ Convers Manage, 108 (2016) 190-201.

500      [14] C.L. Yan, A. Yang, I.L. Chien, S.A. Wei, W.F. Shen, J.Z. Ren, Advanced exergy

501      analysis of organic Rankine Cycles for Fischer-Tropsch syngas production with

502      parallel dry and steam methane reforming, Energ Convers Manage, 199 (2019)

503      111963.

504      [15] G. Li, Z.Y. Liu, F. Liu, B. Yang, S.Q. Ma, Y.J. Weng, Y.L. Zhang, Y.T. Fang,

505      Advanced exergy analysis of ash agglomerating fluidized bed gasification, Energ

506      Convers Manage, 199 (2019) 111952.

507      [16] Z. Mohammadi, M. Fallah, S.M.S. Mahmoudi, Advanced exergy analysis of

508      recompression supercritical CO2 cycle, Energy, 178 (2019) 631-643.

509      [17] S.R. Sun, W. Chun, A. Yang, W.F. Shen, P.Z. Cui, J.Z. Ren, The separation of

510      ternary azeotropic mixture: Thermodynamic insight and improved multi-objective

511      optimization, Energy, 206 (2020) 118117.

512      [18] F. Buhler, T.V. Nguyen, J.K. Jensen, F.M. Holm, B. Elmegaard, Energy, exergy

513      and advanced exergy analysis of a milk processing factory, Energy, 162 (2018) 576-

514      592.

515      [19] X. Feng, X.X. Zhu, J.P. Zheng, A practical exergy method for system analysis, Proc

516      Iecec, (1996) 2068-2071.

517      [20] Y.N. Zhang, Y.J. Zhao, X.Y. Gao, B.X. Li, J.Q. Huang, Energy and exergy analyses

518      of syngas produced from rice husk gasification in an entrained flow reactor, J Clean

519      Prod, 95 (2015) 273-280.

520      [21] R.J. Zemp, S.H.B. deFaria, M.D.L.O. Maia, Driving force distribution and exergy

521      loss in the thermodynamic analysis of distillation columns, Comput Chem Eng, 21

522      (1997) S523-S528.

523      [22] G. de Koeijer, R. Rivero, Entropy production and exergy loss in experimental

524      distillation columns, Chem Eng Sci, 58 (2003) 1587-1597.

525      [23] H. Benyounes, W.F. Shen, V. Gerbaud, Entropy Flow and Energy Efficiency

526      Analysis of Extractive Distillation with a Heavy Entrainer, Ind Eng Chem Res, 53

527      (2014) 4778-4791.

528      [24] J. Galindo, S. Ruiz, V. Dolz, L. Royo-Pascual, Advanced exergy analysis for a

529      bottoming organic rankine cycle coupled to an internal combustion engine, Energ

530      Convers Manage, 126 (2016) 217-227.

531      [25] A. Bejan, G. Tsatsaronis, M. Moran. Thermal design and optimization[J].

532      Astrophysics, 1996, 1(4).

533 [26] A. Lazzaretto, G. Tsatsaronis, SPECO: A systematic and general methodology for
534     calculating efficiencies and costs in thermal systems, Energy, 31 (2006) 1257-1289.

535 [27] T. Morosuk, G. Tsatsaronis, M. Schult, Conventional and Advanced Exergetic
536     Analyses: Theory and Application, Arabian Journal for Science and Engineering,
537     38 (2012) 395-404.

538 [28] M. Mehrpooya, M.M.M. Sharifzadeh, H. Ansarinasab, Investigation of a novel
539     integrated process configuration for natural gas liquefaction and nitrogen removal
540     by advanced exergoeconomic analysis, Appl Therm Eng, 128 (2018) 1249-1262.

541 [29] Z.Q. Wei, B.J. Zhang, S.Y. Wu, Q.L. Chen, G. Tsatsaronis, Energy-use analysis
542     and evaluation of distillation systems through avoidable exergy destruction and
543     investment costs, Energy, 42 (2012) 424-433.

544 [30] T. Morosuk, G. Tsatsaronis, A new approach to the exergy analysis of absorption
545     refrigeration machines, Energy, 33 (2008) 890-907.

546 [31] Z. Liu, B. Liu, J.Z. Guo, X. Xin, X.H. Yang, Conventional and advanced exergy
547     analysis of a novel transcritical compressed carbon dioxide energy storage system,
548     Energ Convers Manage, 198 (2019) 111807.

549 [32] T. Morosuk, G. Tsatsaronis, C.Y. Zhang, Conventional thermodynamic and
550     advanced exergetic analysis of a refrigeration machine using a Voorhees'
551     compression process, Energ Convers Manage, 60 (2012) 143-151.

552 [33] K. Rahbar, S. Mahmoud, R.K. Al-Dadah, N. Moazami, S.A. Mirhadizadeh,
553     Review of organic Rankine cycle for small-scale applications, Energ Convers
554     Manage, 134 (2017) 135-155.

555 [34] H.S. Yu, X. Feng, Y.F. Wang, Working Fluid Selection for Organic Rankine Cycle
556     (ORC) Considering the Characteristics of Waste Heat Sources, Ind Eng Chem Res,
557     55 (2016) 1309-1321.

558 [35] N.B. Desai, S. Bandyopadhyay, Process integration of organic Rankine cycle,
559     Energy, 34 (2009) 1674-1686.

560 [36] J.H. Holland, Adaptation in natural and artificial systems: an introductory analysis
561     with applications to biology, control, and artificial intelligence, The MIT Press,
562     1992.

563 [37] Y. Su, S.M. Jin, X.P. Zhang, W.F. Shen, M.R. Eden, J.Z. Ren, Stakeholder-oriented
564     multi-objective process optimization based on an improved genetic algorithm,
565     Comput Chem Eng, 132 (2019) 106618.

566 [38] C.L. Yan, L.P. Lv, S.A. Wei, A. Eslamimanesh, W.F. Shen, Application of

retrofitted design and optimization framework based on the exergy analysis to a crude oil distillation plant, Appl Therm Eng, 154 (2019) 637-649.

[39] X.X. Gao, Q. Gu, J.Q. Ma, Y.F. Zeng, MVR heat pump distillation coupled with ORC process for separating a benzene-toluene mixture, Energy, 143 (2018) 658-665.

[40] H.S. Yu, J. Eason, L.T. Biegler, X. Feng, Simultaneous heat integration and techno-economic optimization of Organic Rankine Cycle (ORC) for multiple waste heat stream recovery, Energy, 119 (2017) 322-333.

[41] T. Shi, A. Yang, S.M. Jin, W.F. Shen, S.A. Wei, J.Z. Ren, Comparative optimal design and control of two alternative approaches for separating heterogeneous mixtures isopropyl alcohol-isopropyl acetate water with four azeotropes, Sep Purif Technol, 225 (2019) 1-17.

[42] H. Zhou, Y. Cai, F. You, Systems Design, Modeling, and Thermoeconomic Analysis of Azeotropic Distillation Processes for Organic Waste Treatment and Recovery in Nylon Plants, Ind Eng Chem Res, 57 (2018) 9994-10010.

[43] Q.J. Zhang, S.J. Yang, P.Y. Shi, W. Hou, A.W. Zeng, Y.G. Ma, X.G. Yuan, Economically and thermodynamically efficient heat pump-assisted side-stream pressure-swing distillation arrangement for separating a maximum-boiling azeotrope, Appl Therm Eng, 173 (2020) 115225.

[44] M.C. Simpson, M.A. Chatzopoulou, O.A. Oyewunmi, N. Le Brun, P. Sapin, C.N. Markides, Technoeconomic analysis of internal combustion engine - organic Rankine cycle systems for combined heat and power in energy-intensive buildings, Appl Energ, 253 (2019) 113462.